Materials Today Bio 31 (2025) 101472

Contents lists available at ScienceDirect

Materials Today Bio

journal homepage: www.journals.elsevier.com/materials-today-bio

Rapid isolation and recovery of *Salmonella* using hollow glass microspheres coated with multilayered nanofilms

Rutwik Joshi [a], Hesaneh Ahmadi [a], Md Nayeem Hasan Kashem [a], Fariha Afnan [a], Siva Parameswaran [b], Chau-Chyun Chen [a], Gizem Levent [c,d,**], Wei Li [a,*]

[a] Department of Chemical Engineering, Texas Tech University, Lubbock, TX, USA
[b] Department of Mechanical Engineering, Texas Tech University, Lubbock, TX, USA
[c] School of Veterinary Medicine, Texas Tech University, Amarillo, TX, USA
[d] Department of Veterinary Integrative Biosciences, Texas A&M University, College Station, TX, USA

A B S T R A C T

Timely isolation, recovery, and identification of *Salmonella* from food samples is essential for prevention and control of foodborne *Salmonella* outbreaks. Traditional culture-based *Salmonella* isolation and serotyping techniques are time consuming and labor intensive. Despite the progress of innovative microfluidic or immunomagnetic isolation techniques, sophisticated lab equipment and microfabrication are often needed. Here, we present a novel, rapid yet simple method for isolation and recovery of *Salmonella* from mixed bacterial populations in food matrices and blood. This method utilizes self-floating hollow glass microspheres (HGMS) coated with biodegradable layer-by-layer (LbL) films and *Salmonella* specific antibodies. The isolation and recovery process can be completed in less than 2 h, without any sophisticated laboratory equipment or external force. In this study, we demonstrate that *Salmonella* can be captured due to antigen-antibody interactions on the surface of HGMS, allowing them to float to the top. The HGMS can then be washed and subjected to enzymatic degradation of the LbL film to recover the captured bacteria. The recovered *Salmonella* can subsequently be grown on selective agar plates for further analysis. Recovery efficiency of up to 22 % and detection limit of 100 CFU/mL were achieved. This method is expected to provide a viable alternative to traditional isolation techniques, especially in resource limited areas.

1. Introduction

Foodborne bacterial infections are responsible for around 3000 mortalities each year in the United States according to Centers for Disease Control and Prevention (CDC) [1]. *Salmonella* is one of the leading causes of these foodborne illnesses. It causes 1.35 million infections, 26,500 hospitalizations and 420 deaths annually in the USA [2]. Food products of animal origin can cause *Salmonella* outbreaks if they are not cooked to the recommended temperatures [3]. Additionally, consuming uncooked vegetables, seeds, and fruits contaminated with farm soil or water can also be sources of food-related *Salmonella* outbreaks [4]. Most *Salmonella* outbreaks are subtype-dependent [5], making subtype identification essential for investigating and understanding the source and distribution of outbreaks. Among the over 2600 serotypes, a few predominant ones are responsible for human outbreaks. Typhimurium, Enteritidis, Newport, and Heidelberg serotypes are the primary causes of *Salmonella* outbreaks, often linked to poultry, eggs, pork, and beef products (NORS, 1971–2021) [6]. Investigating the epidemiology of *Salmonella* serotypes is critical for understanding their pathogenicity, especially given their close association with antibiotic resistance patterns [7,8]. In the USA, *Salmonella* surveillance is conducted by the CDC and United States Department of Agriculture (USDA), Food Safety and Inspection Service (FSIS) laboratories focusing on clinical human cases and routine testing of animal sources and food products. These labs mainly utilize pre-enrichment media and selective *Salmonella* cultures to increase the limit of detection [9], which results in 4–5 days for the whole process [10]. After isolation, isolates are often confirmed using Matrix-Assisted Laser Desorption–Ionization Time-of-Flight Mass Spectrometry (MALDI-TOF) [11]. After species-level confirmation, serotype-level *Salmonella* identification is often required and performed using serum slide-agglutination test, polymerase chain reaction (PCR) [12], Enzyme-Linked Immunosorbent Assay (ELISA) [13], pulsed-field gel electrophoresis (PFGE), and in-silico typing using whole-genome sequencing data. These methods are time-consuming, require trained staff, advanced equipment, and are not cost-effective [9,14].

Considering the scale of public health risk associated with *Salmonella* infections attributed to certain serotypes, development of a rapid, low cost and easily accessible *Salmonella* isolation and serotype confirmation

* Corresponding author.
** Corresponding author. School of Veterinary Medicine, Texas Tech University, Amarillo, TX, USA.
E-mail addresses: Gizemlevent@tamu.edu (G. Levent), wei.li@ttu.edu (W. Li).

https://doi.org/10.1016/j.mtbio.2025.101472
Received 29 September 2024; Received in revised form 19 December 2024; Accepted 8 January 2025
Available online 10 January 2025

method is essential [15]. Exciting new *Salmonella* detection techniques such as fluorescence identification [16,17], surface enhanced Raman scattering [18], colorimetric detection [19] coupled with immunomagnetic separation (IMS), microfluidic separation [20] have been reported, but most of those platforms require sophisticated microfabrication, are labor intensive and require specialized equipment [21,22]. In recent years, magnetic nano/microparticles (MPs) with functionalized antibodies became popular for isolating and detecting bacteria and rare cells [16,23–25]. However, these MPs can negatively affect bacterial cell viability [26], hindering further analyses [26]. Our previous studies [27,28] demonstrated that using self-floating hollow glass microspheres (HGMS), coated with nano-structured biopolymers linked to cancer-specific antibodies, was a promising strategy for isolating cancer cells in human blood [29]. HGMS demonstrated quick capture, ultrahigh capture efficiency, and low limit of detection for commonly used cancer cell lines such as MCF7, SK-BR-3, PC-3, A549 and CCRF-CEM. Remarkably, the whole capture and recovery process was ~30 min without requiring specialized lab instruments or external magnetic sources [27–29]. This rapid and cost-effective method provides a potential solution for targeted cell isolation in settings with low resources.

Herein, we have utilized the HGMS with multilayered nanofilm coating for efficient *Salmonella* isolation and recovery. As depicted in Fig. 1, self-floating HGMS are coated with layer-by-layer (LbL) polymeric nanofilms and conjugated with *Salmonella* specific antibodies. When mixed with bacterial suspension, *Salmonella* are captured due to interaction between antibodies on HGMS surface and the antigen on the surface of *Salmonella.* As HGMS with captured *Salmonella* float to the top of the suspension and separated from rest of the matrix, *Salmonella* are released and recovered through non-invasive enzymatic degradation of the LbL polymeric nanofilms on HGMS, which can be cultured for further downstream analysis. This entire process takes less than 2 h for isolation, recovery of targeted *Salmonella* serotypes and takes less than 24 h for confirmation, compared to the 4–5 days using conventional methods [30]. Additionally, this method can be easily coupled with next-generation sequencing for genomic profiling of targeted *Salmonella* serotypes. Specifically, we have demonstrated isolation and recovery of *Salmonella* Typhimurium from various food and body fluid matrices such as phosphate buffer saline (PBS), beef, cantaloupe, and blood. We have included characterization of LbL nanofilm formation and degradation, simulation of the motion of HGMS on a rotating mixer, investigation of non-specific binding of bacteria and specific capture of *Salmonella* in mixed population with *Pseudomonas aeruginosa* and detection by fluorescence. We were able to achieve recovery of up to 22 % and a detection limit of 100 CFU/mL. Owing to its efficient, rapid, and reliable operation technique coupled with rapid growth of *Salmonella*, this HGMS-mediated isolation and recovery method is a promising alternative to conventional isolation method, especially in resource limited areas.

2. Materials and methods

2.1. Materials

Alginate (ALG) (Pronova, UPLVG, 60 % guluronate, 40 % mannuronate, Mw = 75–200 kDa) was purchased from Novamatrix, Norway. Polydiallyldimethylammonium chloride (PDDA) and alginate lyase were purchased from Sigma-Aldrich without further purification. Biotin hydrazide, 1-Ethyl-3-(3-dimethylaminopropyl) carbodiimide (EDC), sulfo-N-hydroxysuccinimide (sulfo-NHS) (24510), neutravidin (Mw = 60,000 Da), neutravidin Texas Red conjugate (A-2665) (Mw = 200,000–350,000), ampicillin and *Salmonella* Polyclonal Antibody, Biotin (PA1-73022) were purchased from ThermoFisher Scientific. Gentamicin was purchased from Lonza, USA. Difco® nutrient agar and Difco® *Pseudomonas* isolation agar was purchased from BD Bioscience. LB broth, miller was purchased from Fisher Scientific. Hollow glass microspheres (HGMS, density 0.6 g/mL and particle size 18 μm) were purchased from 3M, USA. Blood from healthy donors was purchased from BioreclamationIVT and used within 3 days of collection. All other chemicals were purchased from Sigma-Aldrich. Biotin conjugated ALG (BALG) was prepared following previously published methods [31] as described in supporting information.

2.2. Assembly of LbL nanofilm on HGMS

BALG and PDDA were dissolved in deionized water (pH 7) to a

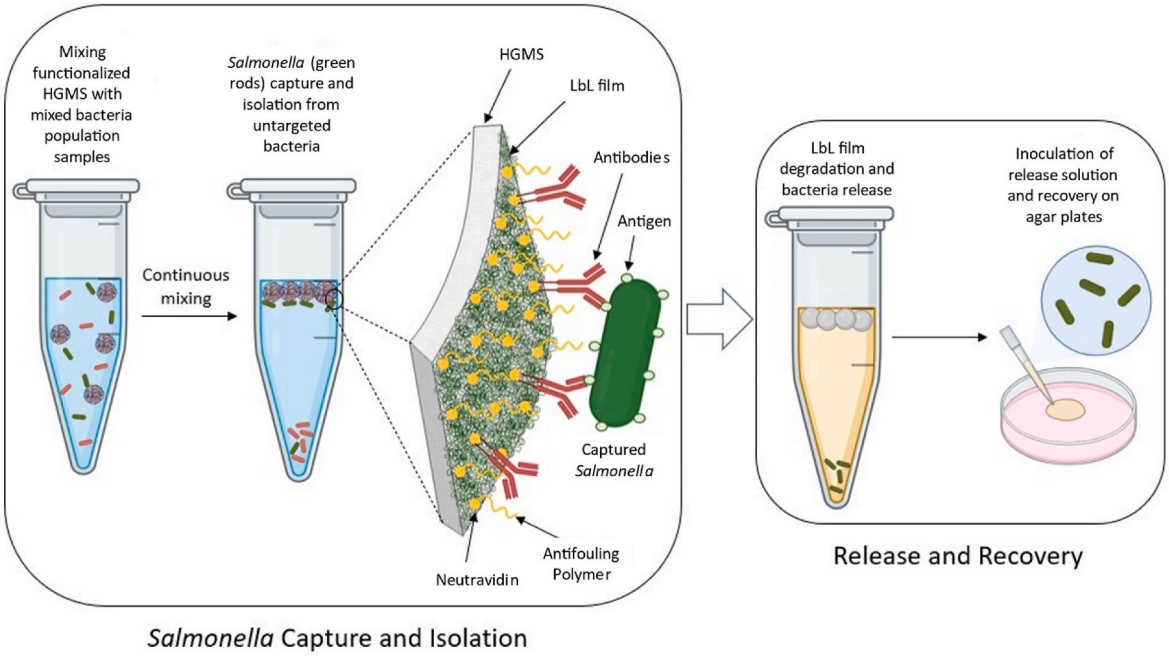

Fig. 1. Schematics of the process of *Salmonella* isolation and enzymatic degradation-mediated recovery using HGMS coated with polymeric nanofilms and specific antibodies.

concentration of 2 mg/mL and subsequently pH was adjusted to 5 using 0.1M sodium hydroxide (NaOH) and 0.1M hydrochloric acid (HCL). HGMS were sterilized with ethanol and washed with deionized water. The deposition of polymers via LbL method involved incubating HGMS with PDDA and BALG polymers for 10 min for the first bilayer and 5 min for each subsequent bilayer, totaling 5 bilayers. All the LbL coating steps were performed at room temperature. A washing step with deionized water was conducted in between each polymer deposition. HGMS were separated from polymer and washing solutions by letting them float to the top of these solutions. Then the solutions were carefully removed from the collecting vials using a pipette leaving HGMS behind and the new solution was introduced.

2.3. Neutravidin, biotinylated poly (ethylene glycol) and anti-Salmonella antibodies modification of layer-by-layer film

After LbL surface modification, the coated HGMS were incubated with 100 μg/mL solution of neutravidin for 12 h. Subsequently, the HGMS were washed with PBS three times before being introduced with a 100 μg/mL solution of *Salmonella* polyclonal antibody to coat the neutravidin functionalized surface. For experiments with spiked lysed blood, 1:1 concentration of *Salmonella* polyclonal antibody and poly (ethylene glycol) (PEG) was used for HGMS surface functionalization to inhibit non-specific binding of blood cells which may lead to blocking of *Salmonella* binding sites.

2.4. Quartz crystal microbalance with dissipation monitoring

LbL deposition of polymeric nanofilms, antibody functionalization, *Salmonella* capture and release were monitored by quartz crystal microbalance with dissipation monitoring (QCM-D) (Q-Sense E4 model). Frequency and dissipation changes were recorded at different overtones (n = 3, 5, 7, 9 and 11) with gold coated AT-cut (Q-Sense, QSX 301) crystals as substrate. The substrate was exposed to oxygen plasma for 5 min at high exposure before use. For LbL deposition, 2 mg/mL solutions of PDDA and BALG were introduced into the QCM-D flow cell for 5 min, with 5 min of rinse step with deionized water in between the polymers. Neutravidin (0.1 mg/mL) and biotinylated antibodies (0.1 mg/mL) were then introduced sequentially for 15 min each with PBS washing of 5 min in between. After antibody functionalization, *Salmonella* Typhimurium suspension was introduced into the cell to evaluate the capture performance. All the liquids were introduced in the QCM-D flow cell at a flow rate of 0.1 mL/min.

The software QTools (version: 3.1.30.624) was used to estimate adsorption and degradation processes based on the Voigt-based viscoelastic model generally used for soft and hydrated polymeric films and protein deposition [32]. The following formulas for frequency and dissipation changes were used for the calculation –

$$\Delta F \approx -\frac{1}{2\pi\rho_0 h_0}\left\{\frac{\eta_3}{\delta_3}+\sum_{j=k}\left[h_j\rho_j\omega-2h_j\left(\frac{\eta_3}{\delta_3}\right)^2\frac{\eta_j\omega^2}{{\mu_j}^2+\omega^2{\eta_j}^2}\right]\right\}$$

$$\Delta D \approx \frac{1}{2\pi f\rho_0 h_0}\left\{\frac{\eta_3}{\delta_3}+\sum_{j=k}\left[2h_j\left(\frac{\eta_3}{\delta_3}\right)^2\frac{\eta_j\omega}{{\mu_j}^2+\omega^2{\eta_j}^2}\right]\right\}$$

where, for a total of k viscoelastic layers under a bulk Newtonian fluid, ρ_0 and h_0 are the density and thickness of the quartz crystal, η_3 is the viscosity of the bulk fluid, δ_3 is the viscous penetration depth of the shear wave in the bulk fluid, ρ_3 is the density of liquid, μ is the elastic shear modulus of an overlayer, and ω is the angular frequency of the oscillation. The pressure of 0.001 Pa s was assumed as liquid viscosity and 1050 kg/m^3 was used as film density. The liquid density was kept at 1010 kg/m^3. Four overtones (3rd, 5th and 7th) were used for mass change calculations.

2.5. Surface morphology and topography by atomic force microscopy (AFM)

The surface morphology and topography of the LbL films at various stages were determined by Bruker Dimension Icon AFM with ScanAsyst. The LbL films were developed with silicon wafer as substrate, since it is not feasible to scan curved micronscale surface of HGMS. 3 similar substrates were coated with 5 layers of LbL films as described previously. After LbL deposition, the surface was functionalized with neutravidin and anti-*Salmonella* antibodies for capture. Two functionalized substrates were dipped in *Salmonella* (10^9 CFU/mL) suspension for 2 h to ensure capture by antigen-antibody interaction. After capture one substrate was dipped in alginate lyase for 30 min for LbL film degradation and *Salmonella* release, while other substrate with captured *Salmonella* was dipped in 2.5 % glutaraldehyde solution for 2 h for fixation. All three substrates were air dried at room temperature overnight before AFM scanning. The tip of AFM was placed on the uniform film areas in tapping mode for imaging.

2.6. Fluorescence imaging

All fluorescence images were taken using Olympus BX53 fluorescence microscope with a U-HGLGPS light source. 4′,6-diamidino-2-phenylindole (DAPI), green fluorescent protein (GFP), Texas Red, and Deep Red images were taken at 345, 488, 530, and 630 nm wavelengths, respectively. All the images were captured with an exposure time of 200 ms.

2.7. Bacterial culture preparation

Liquid cultures of GFP *Salmonella* Typhimurium (ATCC 14028) (resistant to Ampicillin) and mcherry *Pseudomonas aeruginosa* (resistant to Gentamicin) (modified from Dr. Rumbaugh's lab at TTUHSC) were cultured in LB broth with 100 μg/mL ampicillin and 50 μg/mL gentamicin respectively at 37 °C in a shaker incubator for 15h. This bacteria suspension was used to make further serial dilutions in PBS. The exact number of bacteria in a diluted suspension were determined by plating 10 μL on corresponding agar plates (Nutrient agar with 100 μg/mL ampicillin for GFP *Salmonella* Typhimurium and *Pseudomonas* isolation agar with 50 μg/mL gentamicin for *Pseudomonas aeruginosa*). After 20h of incubation at 37 °C, colonies were counted manually using the colony count method to determine colony forming units per milliliter (CFU/mL).

2.8. Scanning electron microscopy

Hollow glass microspheres with and without captured bacteria were characterized by scanning electron microscopy (SEM, Hitachi S-4300, Japan) at 5 kV. HGMS with captured bacteria were fixed with 2.5 % glutaraldehyde solution in cacodylate buffer for 12 h and then washed with cacodylate buffer. After washing, HGMS were treated with 1 % osmium tetroxide (OsO_4) for 30 min followed by 3 washes with deionized water to remove any remaining OsO_4. HGMS in deionized water were flash frozen in liquid nitrogen and lyophilized overnight. The dried samples were iridium-coated with sputter (4 nm) and scanned under SEM at various magnifications.

2.9. Simulation of motion of HGMS

Simulation of motion of HGMS during rotational mixing was performed using laminar flow and particle tracing packages (COMSOL Multiphysics 5.5, COMSOL). The dimensions of the microcentrifuge tube were measured using vernier caliper and a structure with similar dimensions was constructed on AutoCAD (Autodesk AutoCAD 2022). Area occupied by 400 μl of solution was considered for simulation. Theoretically, air-liquid interface was considered as inlet point for HGMS and

their motion was manipulated by rotating mixer. The parameters were defined as follows: particle size was 20 μm and density was defined as 0.6 g/cc, 40,000 particles were introduced at t = 0, surface tension along the walls was defined as 50 N/m, liquid was defined as water and the tube was rotated at 10 rpm. This system was simulated for 60 s which was the time to complete 10 rotations. The simulated area occupied by the HGMS was calculated using Adobe photoshop.

2.10. Cell isolation and recovery

Antibody modified HGMS were mixed with 400 μL of diluted *Salmonella* suspensions (in PBS, diluted beef extract, cantaloupe juice and lysed blood) on a rotating mixer at 10 rpm for 60 min at room temperature. After 60 min of mixing, HGMS were carefully transferred into a new Eppendorf tube and washed with PBS to remove unattached bacteria. Then alginate lyase (400 μL at 1 mg/mL) was added to the washed HGMS to degrade the LbL film and release the captured *Salmonella*. This release solution was platted onto nutrient agar with 100 μg/mL ampicillin for recovery (captured bacteria released after enzymatic degradation of LbL nanofilm) and incubated for 20 h at 37 °C. Colonies on this plate were counted to determine the CFU/mL of the release solution and recovery efficiency of the process. These recovered bacterial colonies were used for fluorescence microscopy for isolate confirmation. Fig. 1 shows the schematic of the capture, release, and recovery process.

The recovery efficiency was calculated using the following formula –

$$\textit{Recovery Efficiency} = \frac{\textit{Concentration of Salmonella in Release Solution}}{\textit{Concentration of Spiked Salmonella}}$$

2.11. Statistical methods

Data analysis was performed between the groups using student's t-test and ANOVA (n = 3) by software Graphpad Prism. Calculated probabilities are indicated as ***p < 0.001, **p < 0.01, *p < 0.05 and NS p > 0.05.

3. Results and discussion

3.1. Preparation and characterization of HGMS coated with LbL nanofilms

HGMS with an average diameter of 20 μm (Fig. S1), were chosen for capture and isolation of *Salmonella* since they have a density (0.6 g/mL) lower than aqueous mediums, hence float to the top when mixed with aqueous medium and can be easily separated. In addition, glass provides a stable substrate with an inherent strong negative charge which makes it easy to coat it with alternate positive and negatively charged LbL polymeric films. This technique of using LbL coated HGMS has been successfully used previously for isolation of circulating tumor cells from blood [27,28,33]. Specifically, 5 bilayers of LbL film were developed on the HGMS surface with PDDA as the positively charged electrolyte and biotin-conjugated alginate as the negatively charged electrolyte as depicted in Fig. 2A. PDDA was chosen as one of the polymers owing to its positively charged nature and proven biocompatibility in previous studies [34]. Alginate was chosen as the negatively charged polymer since it is naturally derived, biocompatible, extensively used, can be enzymatically degraded with alginate lyase at ambient conditions and can be easily modified with biotin conjugation through carbodiimide

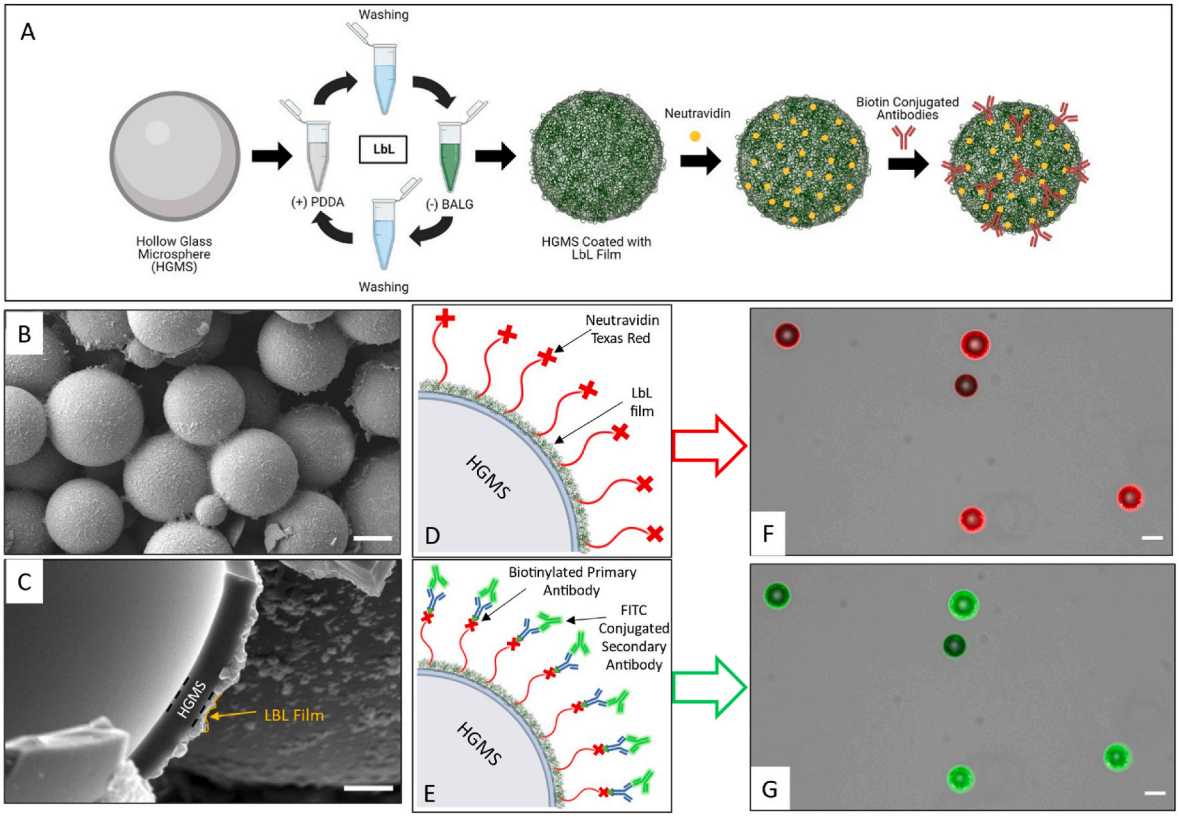

Fig. 2. – (A) Schematic of LbL polymeric coating method for making nanofilms and *Salmonella* antibodies functionalized HGMS for specific capture, isolation and recovery. (B) Scanning electron microscopy (SEM) image of PDDA/BALG nanofilms coated HGMS (scale bar = 10 μm). (C) Cross-sectional SEM image of coated HGMS showing glass substrate (black dashed lines) with LbL film coated on the surface (yellow line) (scale bar = 1 μm). (D) Schematic and (F) fluorescent image depicting binding of neutravidin Texas Red to biotin molecules on the film surface (scale bar = 20 μm). (E) Schematic and (F) Fluorescent image depicting successful functionalization of primary antibodies confirmed by binding of FITC conjugated secondary antibodies (scale bar = 20 μm). (For interpretation of the references to color in this figure legend, the reader is referred to the Web version of this article.)

reaction [31,35,36].

HGMS showed uniform size distribution, good dispersibility and no visible clumping. As seen from the SEM images, LbL coated HGMS had a smooth surface (Fig. 2B) with a nanofilm on the surface (Fig. 2C). Successful deposition of each polymeric layer was also confirmed by QCM-D monitoring (Figure S4 A and B). To verify successful conjugation of biotin to alginate and presence of biotin active sites on the HGMS surface after LbL deposition, fluorescent neutravidin with Texas Red conjugation was introduced after deposition of last bilayer of LbL film (Fig. 2D). Strong red fluorescence, as shown in Fig. 2F, confirmed the successful deposition of LbL film and also the presence of biotin molecules on the surface. This conjugation was also confirmed with increased mass in QCM-D analysis (Fig. 4F). Neutravidin has four biotin binding sites and can accommodate 1–2 biotin molecules [27,37]. Next, biotinylated primary antibodies were introduced after this step for surface functionalization of HGMS. To confirm the successful deposition of these primary antibodies, FITC conjugated IgG secondary antibodies, which can bind to the primary antibodies that were incubated with the functionalized HGMS (Fig. 2E). Successful binding of primary and secondary antibodies was visually confirmed by detection of fluorescence on the HGMS surface under a fluorescence microscope (Fig. 2G).

All these results confirmed the successful deposition of LbL film and antibody functionalization on HGMS surface which could be further used for rapid isolation and recovery of *Salmonella* and various other bacteria.

3.2. Simulation of HGMS motion during capture process

Motion of the HGMS in a collecting vial on a rotator was simulated using COMSOL Multiphysics 5.5 with the parameters mentioned in the Methods section. Fig. 3A shows the schematic of the simulation parameters at t = 0. The simulation was performed for 60 s which corresponds to 10 full rotations at the rotation speed of 10 RPM. As shown in the figure, at t = 0 all the particles were at the top of the tube with a velocity of 0 m/s and covered 0 % area of the liquid in the tube. Fig. 3A also depicts the particle distribution in the microcentrifuge tube at every second of the first rotation. Over the course of time, HGMS dispersed and diffused through the liquid. The total area of the simulated liquid in the 500 μl microcentrifuge tube was around 115.8 mm^2. At t = 1 s, the area covered by HGMS was 61.7 mm^2 which was 53.2 % of the total area and at t = 6 s, i.e. at the end of the first rotation, it was 83.4 mm^2 which was 72.1 % of the total area. All the areas were measured using Adobe Photoshop. Fig. S2 shows the increasing trend of area of coverage by HGMS in one rotation. During the simulation, the principle forces action on HGMS were gravity (*G*), buoyant force (*B*) due to low density and drag force (*D*) due to the liquid. Equation (1) shows the total force (*F*) acting of HGMS during rotational motion. Direction of B is always opposite to G and D, and HGMS move up when F is positive.

$$\overline{F} = \overline{G} + \overline{D} + \overline{B}$$

We further studied the motion of HGMS over higher number of rotations. Fig. 3B shows the area coverage of HGMS with increasing number of rotations. Fig. S3 also shows the length of diffusion of HGMS in the microtube during this time. We observed a steady increase in area coverage of HGMS over the course of 10 rotations. As mentioned earlier, HGMS covered 72.1 % of the total tube area after 1 rotation (t = 6 s), while after 10 rotations (t = 60 s) coverage was 84.1 % with a steady particle velocity of around 0–0.1 m/s. From these results it is clear that HGMS move at low velocities and cover majority of the microtube area throughout the capture process. This is essential to ensure maximum contact between bacteria and antibodies on the surface of HGMS for optimum capture conditions. Increasing the number of HGMS from 40,000 may also aid in higher probability of capture, hence approximately 2 million (5 mg) HGMS were used in every experiment. Movies of laminar flow (velocity profile of liquid during rotational mixing) and particle tracing (motion of HGMS during rotational mixing) are included in supporting information.

3.3. LbL film characterization

I. Over the course of bacteria capture

We studied the LbL film characteristics before and after bacteria capture with AFM, QCM-D and SEM analysis. As shown in Fig. 4A, all the

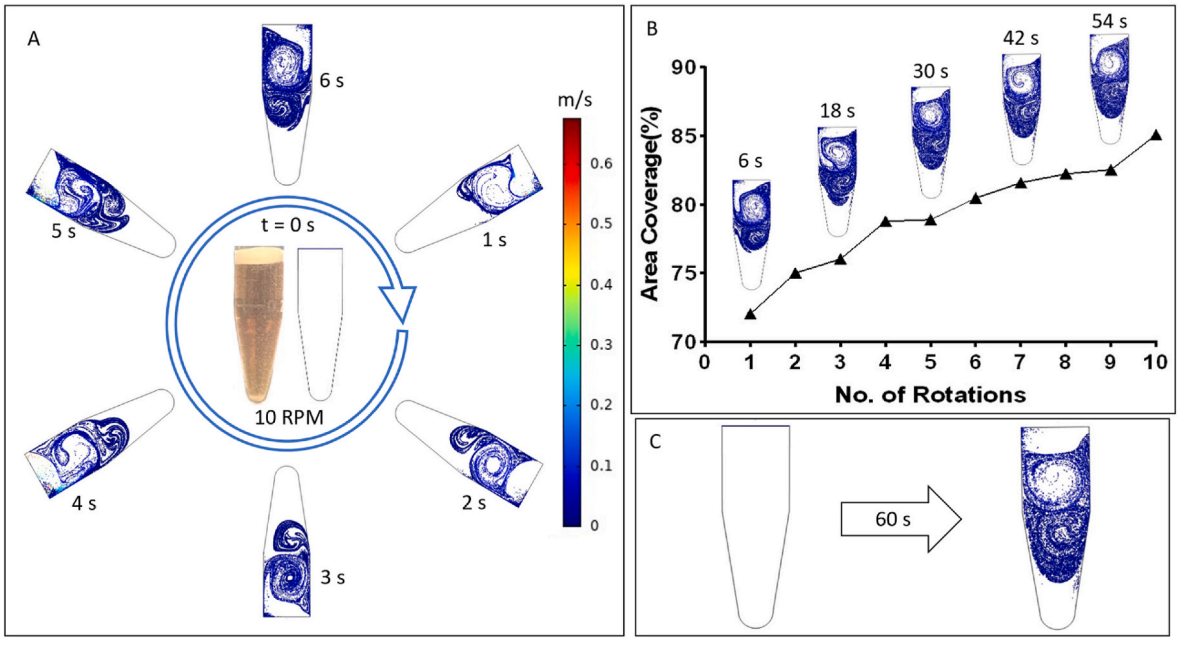

Fig. 3. – Simulation of the motion of HGMS in a collecting vial on a rotator– (A) HGMS dispersion in 400 μL aqueous medium in a microcentrifuge tube at rotation speed of 10 RPM during the first rotation cycle of 6 s (color bar indicates the speed of each particle in meters/second). (B) Plot of percentage of the total liquid area covered by HGMS over 10 rotations (60 s) of rotating at 10 RPM. (C) Images showing HGMS dispersion from t = 0s to t = 60s indicating through mixing of HGMS with the aqueous medium on a rotator. (For interpretation of the references to color in this figure legend, the reader is referred to the Web version of this article.)

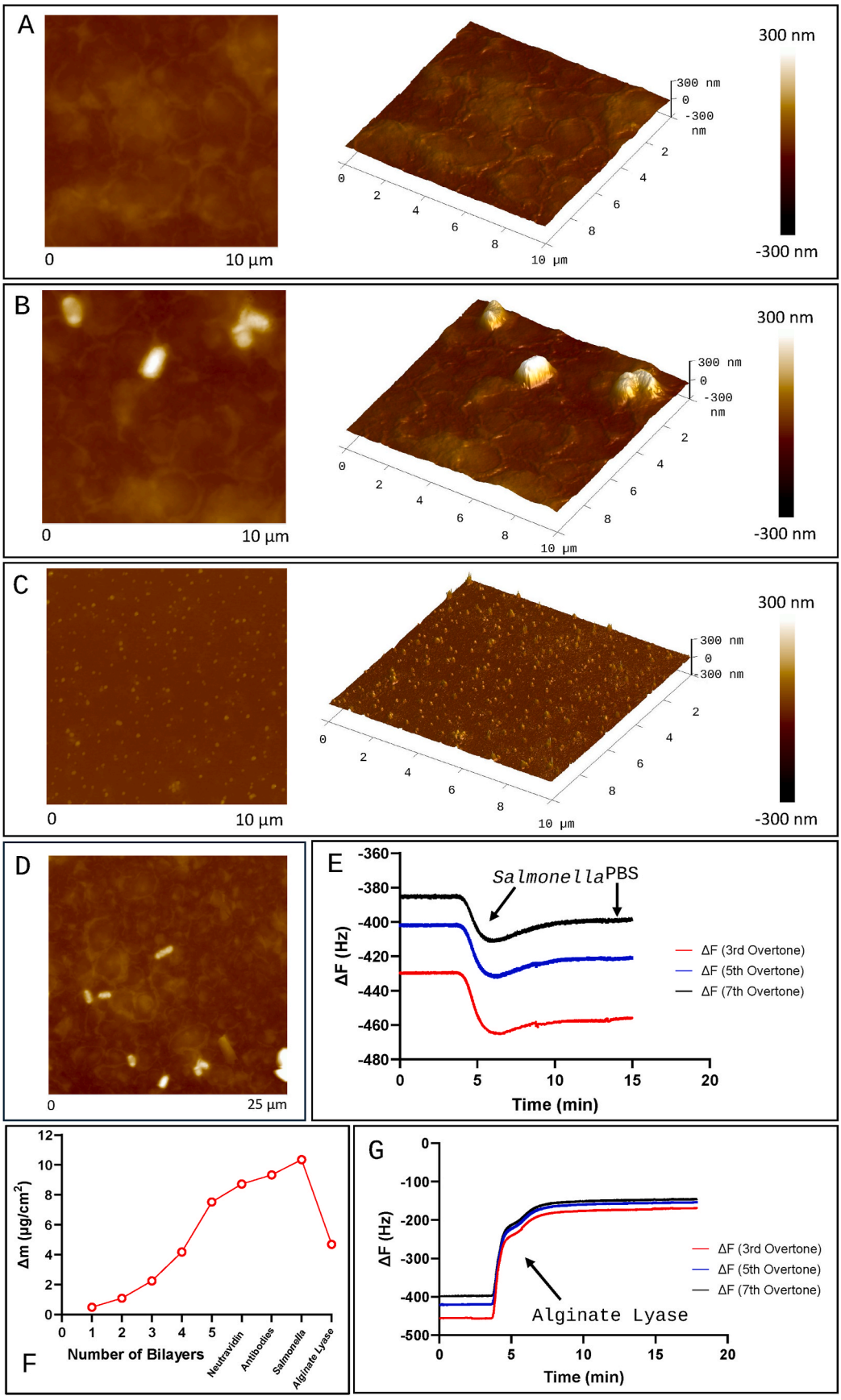

(caption on next page)

Fig. 4. – Characterization of LbL film, bacteria capture and film degradation for bacterial recovery – (A) Atomic force microscopy (AFM) micrograph of $(PDDA/BALG)_5$ LbL film indicating smooth film morphology (color bar indicates the film thickness at various points). (B) AFM micrograph of the antibody functionalized LbL film after capturing *Salmonella* on the surface, confirmed by distinct rod-shaped peaks higher than the normal film surface. (C) AFM micrograph of degraded LbL film showing release of captured *Salmonella* (with no rod-shaped peaks), distinct small peaks with no uniform surface suggesting film degradation. (D) AFM scan after *Salmonella* capture over a wider area of 25 × 25 μm^2. (E) Change in frequency at 3 different overtones after introducing *Salmonella* in QCM-D chamber. (F) Stepwise change in mass deposition during LbL deposition, biotin-neutravidin conjugation, antibody functionalization, *Salmonella* capture and film degradation by alginate lyase enzymatic treatment. (G) Change in frequency after introduction of alginate lyase solution and release of captured *Salmonella* by LbL film degradation. (For interpretation of the references to color in this figure legend, the reader is referred to the Web version of this article.)

AFM samples were scanned over a 10 × 10 μm^2 area. Specifically, LbL film with neutravidin and antibody functionalization had an even film distribution with an RMS roughness of 18.8 nm. After the capture, the RMS roughness increased to 40.9 nm. As shown in Fig. 4B, distinct rod-shaped peaks of *Salmonella* can be seen with heights greater than the bare film. This also gave a visual proof of *Salmonella* captured on the antibody functionalized LbL film as it is challenging to image bacteria on curved HGMS surface with fluorescence or light microscopy.

We also monitored $(PDDA/BALG)_5$ LbL film deposition, functionalization and *Salmonella* capture using QCM- D. The amount of mass deposited on the substrate per cm^2 during film formation and mass added by *Salmonella* capture was estimated using this method. In QCM-D, decrease in resonance frequency (*F*) corresponds to increase in mass adsorption on the sensor substrate, while increase in F corresponds to desorption or removal of loosely bound mass. Dissipation (*D*) represents the viscoelastic behavior of the adsorbed mass, increase in D corresponds to adsorption of softer or more elastic mass on the sensor substrate. Figure S4 A and B show a stepwise decrease in *F* and increase in *D* during the 5 bilayers of LbL film adsorption indicating increase in soft LbL film formation. These changes in *F* and *D* can be used to calculate the mass adsorbed on the substrate using Voigt model. The LbL film added around 7.53 $\mu g/cm^2$ to the substrate indicating successful adsorption of polymeric layers (Fig. 4F). After polymer deposition, neutravidin and biotin-conjugated *Salmonella* polyclonal antibodies were introduced into the chamber for 15 min each. Figure S5 A and B and Figure S6 A and B show the decrease in *F* and increase in *D* after introducing neutravidin and *Salmonella* antibodies respectively. According to Voigt-based viscoelastic model calculations, neutravidin added approximately 1.2 $\mu g/cm^2$ mass to the film which corresponds to the surface density of 1.2 × 10^5 neutravidin molecules/μm^2. Since neutravidin can bind to 1–2 biotin molecules, the PDDA/BALG film had at least 1.2 × 10^5 biotin molecules/μm^2 before neutravidin deposition. After neutravidin deposition, a few more biotin binding sites become available for attachment of biotin conjugated antibodies. The antibodies added another 610 ng/cm^2, which corresponds to the density of 2.45 × 10^4 antibodies/μm^2. This antibody density has been proven to cover the entire surface of beads and sufficient for capturing cells [27,34,38]. After antibody functionalization, *Salmonella* suspension was introduced (*F* and *D* changes indicated in Fig. 4E and Figure S7 A respectively), which resulted in an increase of 1.02 $\mu g/cm^2$ in mass. This mass change corresponds to deposition of approximately 10^6 cells/cm^2 if we consider mass of 1 bacterium to be 10^{-12} g.

II. After degradation and bacterial release

We also characterized the LbL film after degradation with alginate lyase (1 mg/mL). Evaluating the surface morphology of the substrate and monitoring the mass change during LbL film degradation is essential to understand bacteria release and recovery. As seen from Fig. 4C, the height in the AFM micrograph reduced dramatically with intermediate short peaks indicating film degradation of the top layers. The RMS roughness reduced to 10.2 nm from 18.8 nm (bare film) and 40.9 nm (film with captured bacteria) indicating successful release of captured *Salmonella* with the film. Release was also confirmed from the AFM height profiles from these 3 different stages as the height increased when bacteria were captured in the film (Fig. 4B) and it reduced suddenly showing several peaks on the surface after alginate lyase treatment (Fig. 4C). This reduction in height and appearance of peaks also indicated degradation of the top layers of the LbL film and release of bacteria. QCM-D analysis also revealed a sharp increase in *F* and decrease in *D* as shown in Fig. 4G and S7B respectively. This indicated the desorption of LbL film layers and resulted in reduction in mass (Fig. 4E) from 10.36 $\mu g/cm^2$ to 4.69 $\mu g/cm^2$. This also indicated successful release of captured *Salmonella* after alginate lyase mediated LbL film degradation.

3.4. Capture, release and recovery

I. Pure and mixed culture in PBS

The capture ability of the developed functional HGMS was first tested in spiked PBS at various concentrations. The optimal capture time was studied at 15, 30, 60 and 120 min intervals. 1000 CFU/mL of *Salmonella* were spiked in PBS and mixed with antibody functionalized HGMS. The final concentration of recovered bacteria increased with an increase in capture time from 15 min to 60 min. At 15 min it was 23.3 ± 9.4 CFU/mL and it reached maximum at 60 min to 123.3 ± 20.6 CFU/mL. Further increasing capture time to 120 min caused the drop of bacterial concentration to 110.0 ± 14.1 CFU/mL (Fig. 5A). The drop may be attributed to prolonged exposure to shear forces due to motion of HGMS in the liquid resulting in dislodgement of captured bacteria. Hence, 60 min capture duration was used for all the further experiments.

To check the non-specific binding of the film, experiments were performed with two groups of HGMS. The first group of HGMS had antibody functionalization (Ab), while the other group was without antibody coating (NA). In the first set of experiments, only a single population of bacteria, *Salmonella* in this case, were spiked in PBS at various concentrations from 10,000 CFU/mL to 100 CFU/mL. As shown in Fig. 5B, after release the bacterial concentration for the Ab group was significantly higher than the No Ab group. This established minimal non-specific binding of *Salmonella* to the LbL film in absence of antibody coating.

We also checked the specificity of the capture process towards *Salmonella* by spiking mixed bacterial populations in PBS. *Pseudomonas aeruginosa* were spiked in equal concentrations along with *Salmonella* in PBS at various concentrations. As shown in Fig. 5C, *Pseudomonas aeruginosa* showed negligible attachment, both with antibody and without antibody groups. *Salmonella,* on the other hand, showed significantly higher capture with antibody functionalization as compared to without antibody and *Pseudomonas* at the same spiked concentration. A similar trend was observed even at the low spike concentration of 500 CFU/mL. This established the specificity of the capture process towards *Salmonella*.

In summary, these studies established the capability of HGMS platform in isolation and recovery of specific bacterial population, at concentrations as low as 100 CFU/mL (Fig. S11). Recovery at 100 CFU/mL was significantly lower which can be attributed to lower probability of contact between HGMS and bacterial cell. In the following sections, we further assessed the applicability of this platform in complex spiked matrices mimicking real life applications.

II. Salmonella in food matrices and lysed blood samples

At first, we studied application of HGMS in isolation and recovery of *Salmonella* from spiked food matrices. Contaminated fruits [39,40] and

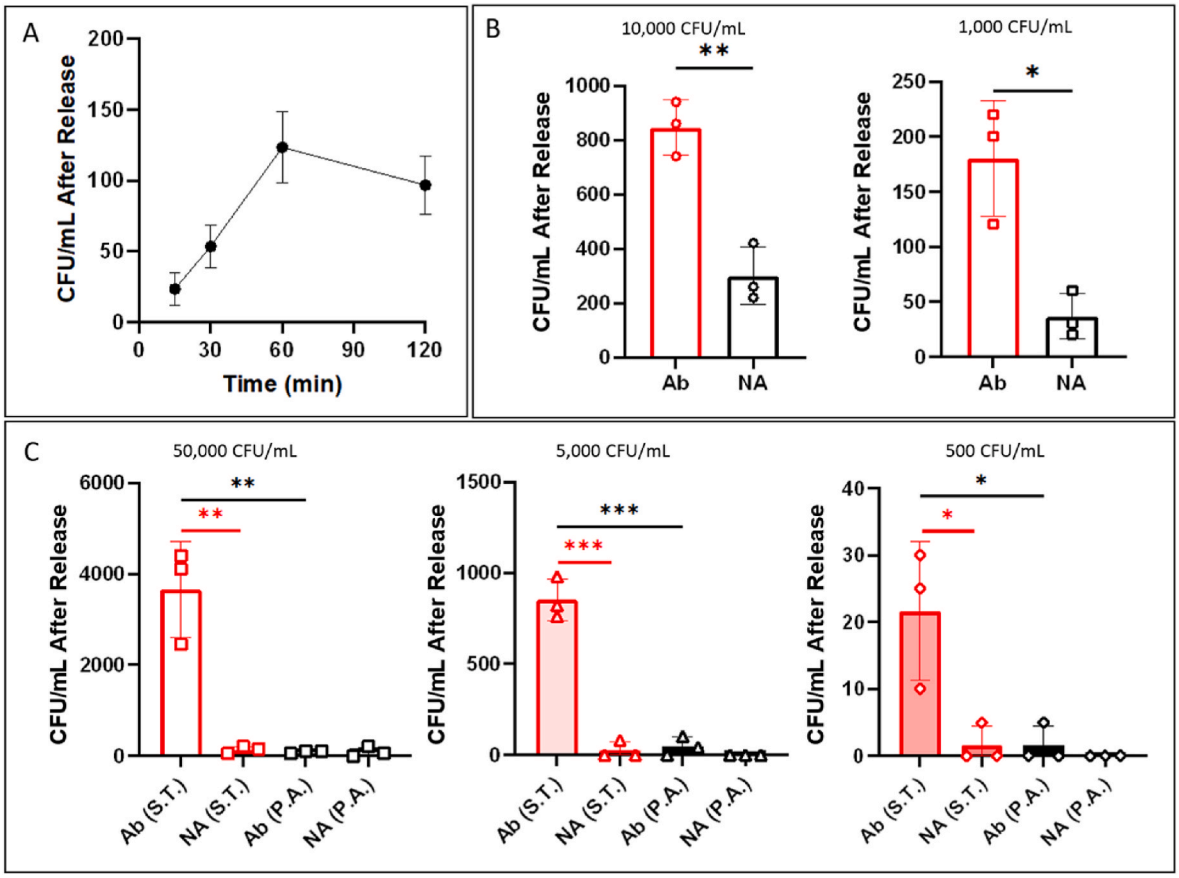

Fig. 5. – *Salmonella* capture and release ability in PBS – (A) Concentration of recovered *Salmonella* with respect to incubation time. (B) Total recovered concentrations in single bacterial population of *Salmonella* at 10,000 and 1000 CFU/mL. (C) Total recovered *Salmonella* concentrations in a mixed bacterial population of *Salmonella* and *Pseudomonas aeruginosa* at 50,000, 5000 and 500 CFU/mL (***p < 0.001, **p < 0.01, *p < 0.05 and NS p > 0.05).

meat products [41,42] generally have a high virulence of *Salmonella*. In this work, cantaloupe and beef were spiked with *Salmonella* at concentration from 50,000 CFU/mL to 200 CFU/mL. Procedure for spiked sample preparation can be found in the Supporting Information and Fig. S12. As described in the previous sections, the same capture and recovery procedures were performed. As shown in Fig. 6A and B, results were similar to that obtained using spiked PBS (shown in Fig. 5C). It is observed that significantly higher recovery in antibody functionalized HGMS group, hinting towards the fact that spiked food matrices do not hinder with the capture process. We were able to establish a slightly higher detection limit of 200 CFU/mL with these spiked matrices (Fig. S13). The higher detection limit as compared to PBS can be attributed to the presence of proteins and fat molecules in the food matrices which may impact the capture due to blockade of *Salmonella* binding sites on the HGMS surface. Fig. 6C shows the floating ability of HGMS in beef extract to capture and isolate bacteria. As seen in the figure, antibody functionalized HGMS capture the spiked *Salmonella* and float to the top leaving other untargeted bacteria, fat molecules, proteins, remaining small meat chunks, etc. in the solution. These floating HGMS can be easily separated from the extract, washed with PBS and subject to LbL film degradation by treatment with alginate lyase for *Salmonella* recovery.

To visualize the captured *Salmonella* on HGMS surface, scanning electron microscopy (SEM) was also performed on fixed bacteria after capture. Fig. 6E depicts the pseudo-colored SEM image of a single HGMS (pseudo-light yellow) with distinct rod-shaped *Salmonella* (pseudo-green) captured on its surface. Fig. 6D shows the colony formation 20 h after *Salmonella* isolation, release, and inoculation for recovery. Recovery with antibody functionalization clearly shows a higher number of colonies 20 h after inoculation on the agar plates. Fig. S14 shows the fluorescent images of recovered *Salmonella* from beef.

Typhoidal and non-typhoidal *Salmonella* infections can also spread into bloodstream and can prove to be fatal [43]. Hence, *Salmonella* isolation and recovery from blood is of great importance. For this purpose, we studied isolation of *Salmonella* from lysed blood samples at 1000 CFU/mL. Procedure for lysed blood preparation can be found in Supporting information. Blood cells are approximately 10 times bigger in size than bacterial cells. These cells can non-specifically bind to LbL film surface due to high protein expression on the surface, electrostatic and hydrophobic interactions [34]. This may result in blocking of bacterial binding sites on HGMS, resulting in lower capture ability. Electrically neutral and hydrophilic polymer coatings such as poly(ethylene glycol) (PEG) can significantly reduce this non-specific binding by inhibiting electrostatic and hydrophobic interactions [44]. We grafted PEG and antibodies in 1:1 ratio after neutravidin modification on HGMS surface. As depicted in Fig. 6F, concentration of released *Salmonella* with PEG + antibodies coating was 146.7 ± 17.0 CFU/mL, which was significantly higher than just antibodies coating (83.3 ± 24.9 CFU/mL).

This system has the potential to be translated into clinical settings for bacteria isolation and detection after further improvements and optimizations in recovery efficiency and detection limit. We envision this system to be used as a kit in clinical set up for bacteria detection in food and body fluids in resource deprived locations. Scaling up the production of LbL coated particles is a challenge, however traditional reactors such as fluidized bed and tangential flow filtration have proved to be efficient for such processes [45]. This method also has an advantage of being cost effective and time saving compared to the traditional methods. After a rough calculation, our approach costs around $5 per

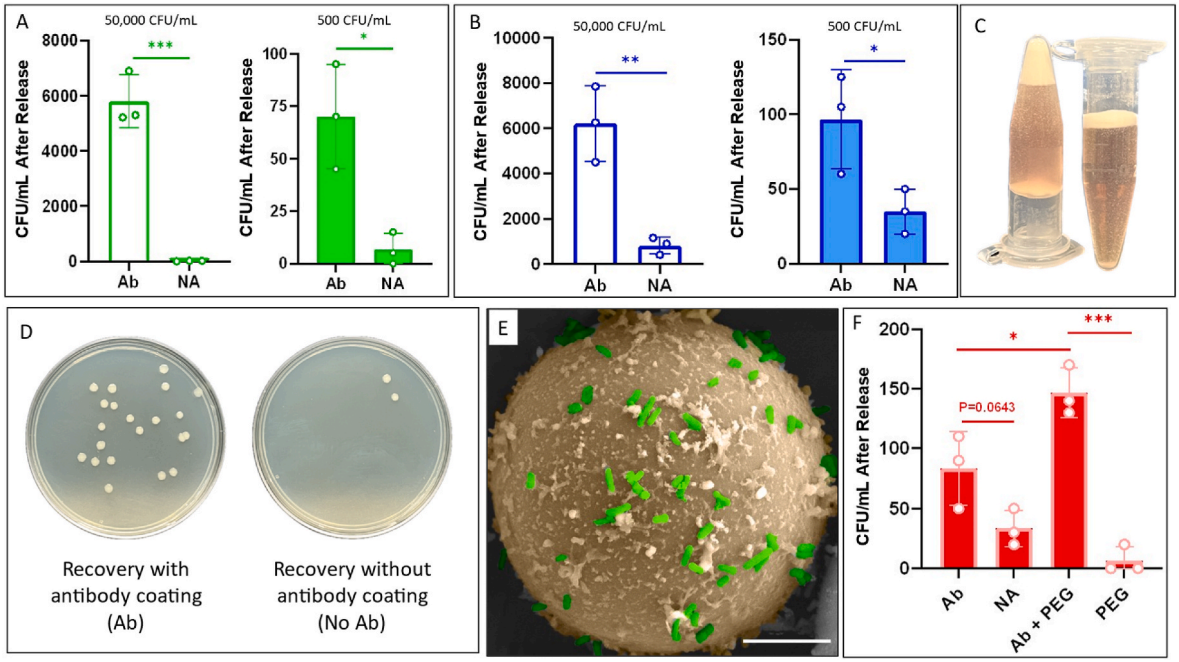

Fig. 6. – Capture and recovery of *Salmonella* in spiked food and blood samples – (A) Capture efficiency in *Salmonella* spiked beef extract at 50,000 and 500 CFU/mL. (B) Capture efficiency in *Salmonella* spiked cantaloupe at 50,000 and 500 CFU/mL. (C) Image of HGMS floating on beef extract in inverted and upright position showing simple separation without any external force. (D) Colony formation 20h after *Salmonella* recovery with and without antibody functionalization (petri dish diameter = 100 mm). (E) Pseudo-colored SEM image of *Salmonella* (pseudo-green colored rod-shaped structured) captured on functionalized HGMS surface (pseudo-yellow colored) (scale bar = 5 μm). (F) Capture efficiency in *Salmonella* spiked lysed blood with and without PEG antifouling layer at 1000 CFU/mL (***$p < 0.001$, **$p < 0.01$, *$p < 0.05$ and NS $p > 0.05$). (For interpretation of the references to color in this figure legend, the reader is referred to the Web version of this article.)

test including the HGMS, polymers, neutravidin, antibodies, alginate lyase, selective agar plate and does not require any electricity or sophisticated lab equipment. Extending this platform to clinical settings may face some challenges such as interference from other good and bad bacterial populations present in the samples. Environmental factors such as pH, contaminants, etc. may also interfere with the process which will need to be addressed in future studies. By selecting other antibodies to target other specific antigens, this platform can be extended to capture bacteria beyond *Salmonella*.

4. Conclusion

In this study, we reported LbL nanofilm and specific antibody-coated self-floating HGMS for rapid isolation and recovery of bacteria, using *Salmonella* Typhimurium as the model organism. The whole process took 2 h for isolation and recovery and we attained a detection limit of 100 CFU/mL in PBS. Moreover, we also demonstrated the capability of our approach in spiked food and blood samples and achieved 200 CFU/mL detection limit, which indicates that it could be potentially translated to clinical applications. Although we have demonstrated the isolation and recovery of *Salmonella* Typhimurium as a model system, this platform can be extended for detection of various bacterial populations that have a significant impact on public health, such as other *Salmonella* serotypes (e.g., Enteritidis, Heidelberg and Newport) or other bacterial species such as shigella-toxin producing E. Coli. To do so, we only need to coat the corresponding antibodies on HGMS surface. The entire process requires no sophisticated lab equipment, trained personnel, or external power, and hence, can be used in resource deficient areas for point-of-care diagnostics. In addition, our method can be readily integrated with molecular techniques such as PCR, Q-PCR and next generation sequencing, for further isolate characterization.

CRediT authorship contribution statement

Rutwik Joshi: Writing – review & editing, Writing – original draft, Visualization, Validation, Software, Methodology, Investigation, Formal analysis, Data curation, Conceptualization. **Hesaneh Ahmadi:** Writing – review & editing, Writing – original draft, Methodology, Data curation. **Md Nayeem Hasan Kashem:** Writing – review & editing, Writing – original draft, Methodology, Data curation. **Fariha Afnan:** Writing – review & editing, Writing – original draft, Methodology, Data curation. **Siva Parameswaran:** Validation, Software, Formal analysis. **Chau-Chyun Chen:** Writing – review & editing, Validation, Supervision, Software, Funding acquisition. **Gizem Levent:** Writing – review & editing, Writing – original draft, Validation, Supervision, Project administration, Methodology, Investigation, Funding acquisition, Conceptualization. **Wei Li:** Writing – review & editing, Writing – original draft, Validation, Supervision, Resources, Project administration, Investigation, Funding acquisition, Formal analysis, Data curation, Conceptualization.

Statement of significance

This is the first reported work on rapid isolation and recovery of *Salmonella* using self-floating hollow glass microspheres coated with multilayered nanofilms and functionalized with specific antibodies. The ability to isolate *Salmonella* in under 2 h from spiked food and blood samples was demonstrated without any sophisticated laboratory equipment or any external force. Recovery of bacteria was achieved non-invasively through enzymatic degradation of the multilayered film. This technique was able to bypass the disadvantages of the traditional isolation methods that are either time consuming or negatively impact the recovered bacteria.

Declaration of competing interest

Authors declare no conflict of interest.

Acknowledgements

Funded through an appointment to the U.S. Department of Agriculture's (USDA) Food Safety and Inspection Service (FSIS) Food Safety Fellowship Program administered by the Oak Ridge Institute for Science and Education (ORISE) through an interagency agreement between the U.S. Department of Energy (DOE) and the National Institute of Environmental Health Sciences. Authors also acknowledge support and contribution of Dr. Isabel Walls from USDA-FSIS.

Appendix A. Supplementary data

Supplementary data to this article can be found online at https://doi.org/10.1016/j.mtbio.2025.101472.

Data availability

Data will be made available on request.

References

[1] Foodborne Germs and Illnesses, Center for Disease Control and Prevention, 2023.
[2] Salmonella, Center for Disease Control and Prevention, 2024.
[3] USDA-FSIS, Fact sheet "Ground beef and Food Safety, Food Safety and Inspection Service, Science and Technology, Microbiology Division D.C, U.S. Department of Agriculture, Washinton, 2016.
[4] M.L. Hutchison, L.D. Walters, A. Moore, K.M. Crookes, S.M. Avery, Effect of length of time before incorporation on survival of pathogenic bacteria present in livestock wastes applied to agricultural soil, Appl. Environ. Microbiol. 70 (2004) 5111–5118.
[5] CDC, An Atlas of *Salmonella* in the United States, 1968-2011, Centers for Disease Control and Prevention, U.S. Department of Health and Human Services, Atlanta, GA, 2013.
[6] CDC-NORS, National Outbreak Reporting System (NORS) Dashboard, Centers for Disease Control and Prevention, U.S. Department of Health and Human Services, Atlanta, GA.
[7] J. Liao, R.H. Orsi, L.M. Carroll, J. Kovac, H. Ou, H. Zhang, M. Wiedmann, Serotype-specific evolutionary patterns of antimicrobial-resistant *Salmonella enterica*, BMC Evol. Biol. 19 (2019) 132.
[8] T.F. Jones, L.A. Ingram, P.R. Cieslak, D.J. Vugia, M. Tobin-D'Angelo, S. Hurd, C. Medus, A. Cronquist, F.J. Angulo, Salmonellosis outcomes differ substantially by serotype, J. Infect. Dis. 198 (2008) 109–114.
[9] R.L. Bell, K.G. Jarvis, A.R. Ottesen, M.A. McFarland, E.W. Brown, Recent and emerging innovations in Salmonella detection: a food and environmental perspective, Microb. Biotechnol. 9 (2016) 279–292.
[10] K.-M. Lee, M. Runyon, T.J. Herrman, R. Phillips, J. Hsieh, Review of Salmonella detection and identification methods: aspects of rapid emergency response and food safety, Food Control 47 (2015) 264–276.
[11] N. Singhal, M. Kumar, P.K. Kanaujia, J.S. Virdi, MALDI-TOF mass spectrometry: an emerging technology for microbial identification and diagnosis, Front. Microbiol. 6 (2015) 791.
[12] J.J. Maurer, Rapid detection and limitations of molecular techniques, Annu. Rev. Food Sci. Technol. 2 (2011) 259–279.
[13] E. de Boer, R.R. Beumer, Methodology for detection and typing of foodborne microorganisms, Int. J. Food Microbiol. 50 (1999) 119–130.
[14] J.W.-F. Law, N.-S. Ab Mutalib, K.-G. Chan, L.-H. Lee, Rapid methods for the detection of foodborne bacterial pathogens: principles, applications, advantages and limitations, Front. Microbiol. 5 (2015).
[15] M. Tietjen, D.Y. Fung, Salmonellae and food safety, Crit. Rev. Microbiol. 21 (1995) 53–83.
[16] C.-Y. Wen, J. Hu, Z.-L. Zhang, Z.-Q. Tian, G.-P. Ou, Y.-L. Liao, Y. Li, M. Xie, Z.-Y. Sun, D.-W. Pang, One-step sensitive detection of Salmonella typhimurium by coupling magnetic capture and fluorescence identification with functional nanospheres, Anal. Chem. 85 (2013) 1223–1230.
[17] J. Hu, Y.-Z. Jiang, M. Tang, L.-L. Wu, H.-y. Xie, Z.-L. Zhang, D.-W. Pang, Colorimetric-fluorescent-magnetic nanosphere-based multimodal assay platform for Salmonella detection, Anal. Chem. 91 (2018) 1178–1184.
[18] H. Kearns, R. Goodacre, L.E. Jamieson, D. Graham, K. Faulds, SERS detection of multiple antimicrobial-resistant pathogens using nanosensors, Anal. Chem. 89 (2017) 12666–12673.
[19] M. Srisa-Art, K.E. Boehle, B.J. Geiss, C.S. Henry, Highly sensitive detection of Salmonella typhimurium using a colorimetric paper-based analytical device coupled with immunomagnetic separation, Anal. Chem. 90 (2018) 1035–1043.
[20] T.N.T. Dao, J. Yoon, C.E. Jin, B. Koo, K. Han, Y. Shin, T.Y. Lee, Rapid and sensitive detection of Salmonella based on microfluidic enrichment with a label-free nanobiosensing platform, Sensor. Actuator. B Chem. 262 (2018) 588–594.
[21] A. Allafchian, S.S. Hosseini, Antibacterial magnetic nanoparticles for therapeutics: a review, IET Nanobiotechnol. 13 (2019) 786–799.
[22] L. Strašák, V.r. Vetterl, J. Šmarda, Effects of low-frequency magnetic fields on bacteria Escherichia coli, Bioelectrochemistry 55 (2002) 161–164.
[23] C.-Y. Wen, Y.-Z. Jiang, X.-Y. Li, M. Tang, L.-L. Wu, J. Hu, D.-W. Pang, J.-B. Zeng, Efficient enrichment and analyses of bacteria at ultralow concentration with quick-response magnetic nanospheres, ACS Appl. Mater. Interfaces 9 (2017) 9416–9425.
[24] J. Chen, B. Park, Effect of immunomagnetic bead size on recovery of foodborne pathogenic bacteria, Int. J. Food Microbiol. 267 (2018) 1–8.
[25] M.I. Pividori, Immunomagnetic Separation of Salmonella with Tailored Magnetic Micro-and Nanocarriers, Salmonella, Springer, 2021, pp. 51–65.
[26] D. Zhang, R.F. Fakhrullin, M. Özmen, H. Wang, J. Wang, V.N. Paunov, G. Li, W. E. Huang, Functionalization of whole-cell bacterial reporters with magnetic nanoparticles, Microb. Biotechnol. 4 (2011) 89–97.
[27] Z. Dong, C.C. Ahrens, D. Yu, Z. Ding, H. Lim, W. Li, Cell isolation and recovery using hollow glass microspheres coated with nanolayered films for applications in resource-limited settings, ACS Appl. Mater. Interfaces 9 (2017) 15265–15273.
[28] Z. Dong, D. Yu, Q. Liu, Z. Ding, V.J. Lyons, R.K. Bright, D. Pappas, X. Liu, W. Li, Enhanced capture and release of circulating tumor cells using hollow glass microspheres with a nanostructured surface, Nanoscale 10 (2018) 16795–16804.
[29] W. Li, Z. Dong, Rapid Cell Isolation and Recovery Using Hollow Glass Microspheres Coated with Biodegradable Nanostructured Films, Google Patents, 2021.
[30] Isolation and Identification of Salmonella from Meat, Poultry, Pasteurized Egg, Siluriformes (Fish) Products and Carcass and Environmental Sponges, Food Safety and Inspection Service, U.S. Department of Agriculture, 2023.
[31] W. Li, E. Reátegui, M.-H. Park, S. Castleberry, J.Z. Deng, B. Hsu, S. Mayner, A. E. Jensen, L.V. Sequist, S. Maheswaran, Biodegradable nano-films for capture and non-invasive release of circulating tumor cells, Biomaterials 65 (2015) 93–102.
[32] K.A. Marx, Quartz crystal microbalance: a useful tool for studying thin polymer films and complex biomolecular systems at the solution− surface interface, Biomacromolecules 4 (2003) 1099–1120.
[33] Y. Yu, Y. Zhang, Y. Chen, X. Wang, K. Kang, N. Zhu, Y. Wu, Q. Yi, Floating immunomagnetic microspheres for highly efficient circulating tumor cell isolation under facile magnetic manipulation, ACS Sens. 8 (2023) 1858–1866.
[34] D. Yu, L. Tang, Z. Dong, K.A. Loftis, Z. Ding, J. Cheng, B. Qin, J. Yan, W. Li, Effective reduction of non-specific binding of blood cells in a microfluidic chip for isolation of rare cancer cells, Biomater. Sci. 6 (2018) 2871–2880.
[35] Q. Li, L. Zheng, Z. Guo, T. Tang, B. Zhu, Alginate degrading enzymes: an updated comprehensive review of the structure, catalytic mechanism, modification method and applications of alginate lyases, Crit. Rev. Biotechnol. 41 (2021) 953–968.
[36] Z. Dong, L. Tang, C.C. Ahrens, Z. Ding, V. Cao, S. Castleberry, J. Yan, W. Li, A benchtop capillary flow layer-by-layer (CF-LbL) platform for rapid assembly and screening of biodegradable nanolayered films, Lab Chip 16 (2016) 4601–4611.
[37] J.R. Wayment, J.M. Harris, Biotin−Avidin binding kinetics measured by single-molecule imaging, Anal. Chem. 81 (2009) 336–342.
[38] C.E. Yoo, H.-S. Moon, Y.J. Kim, J.-M. Park, D. Park, K.-Y. Han, K. Park, J.-M. Sun, W.-Y. Park, Highly dense, optically inactive silica microbeads for the isolation and identification of circulating tumor cells, Biomaterials 75 (2016) 271–278.
[39] I.B. Hanning, J.D. Nutt, S.C. Ricke, Salmonellosis outbreaks in the United States due to fresh produce: sources and potential intervention measures, Foodborne Pathogens and Disease 6 (2009) 635–648.
[40] Salmonella Outbreak Linked to Cantaloupes, Center for Disease Control and Prevention, 2024.
[41] M. Canning, M.G. Birhane, D. Dewey-Mattia, H. Lawinger, A. Cote, L. Gieraltowski, C. Schwensohn, K.A. Tagg, L.K. Francois Watkins, M. Park Robyn, K.E. Marshall, Salmonella outbreaks linked to beef, United States, 2012–2019, J. Food Protect. 86 (2023) 100071.
[42] Salmonella and Ground Beef, Center for Diease Control and Prevention, 2024.
[43] M.J. Worley, Salmonella bloodstream infections, Tropical Medicine and Infectious Disease 8 (11) (2023) 487.
[44] S. Lowe, N.M. O'Brien-Simpson, L.A. Connal, Antibiofouling polymer interfaces: poly (ethylene glycol) and other promising candidates, Polym. Chem. 6 (2015) 198–212.
[45] A. Sarode, A. Annapragada, J. Guo, S. Mitragotri, Layered self-assemblies for controlled drug delivery: a translational overview, Biomaterials 242 (2020) 119929.